

This is a peer-reviewed, accepted author manuscript of the following research article: Fernández-García, R, Walsh, D, O'Connell, P, Domingues Passero, LF, de Jesus, JA, Laurenti, MD, Dea-Ayuela, MA, Ballesteros, MP, Lalatsa, A, Bolás-Fernández, F, Healy, AM & Serrano, DR 2025, 'Targeted oral fixed-dose combination of amphotericin B and miltefosine for visceral leishmaniasis', *Molecular Pharmaceutics*. For the purposes of open access, a CC BY 4.0 licence has been applied to this manuscript.

Targeted Oral Fixed-dose Combination of Amphotericin B- Miltefosine For Visceral Leishmaniasis

Raquel Fernández-García¹, David Walsh², Peter O'Connell², Luiz Felipe Domingues Passero^{3,4}, Jéssica A. de Jesus^{3,4}, Marcia Dalastra Laurenti⁵, María Auxiliadora Dea-Ayuela⁶, M. Paloma Ballesteros^{1,7}, Aikaterini Lalatsa⁸, Francisco Bolás-Fernández⁹, Anne Marie Healy², Dolores R. Serrano^{1,7*}

¹Departamento de Farmacia Galénica y Tecnología Alimentaria. Facultad de Farmacia. Universidad Complutense de Madrid. Plaza de Ramón y Cajal, s/n. 28040 Madrid (Spain)

²School of Pharmacy and Pharmaceutical Sciences. Trinity College Dublin. Dublin 2 (Ireland)

³Institute of Biosciences. São Paulo State University (UNESP). Praça Infante Dom Henrique, s/n. São Vicente 11330-900 (Brazil)

⁴Institute for Advanced Studies of Ocean (IEAMAR). São Paulo State University (UNESP). Rua João Francisco Bendorp, 1178. São Vicente 11350-011 (Brazil)

⁵Laboratório de Patologia das Moléstias Infecciosas (LIM/50). Faculdade de Medicina. Universidade de São Paulo. Avenida Dr. Arnaldo, 455. 01246903 Cerqueira César, São Paulo (Brazil)

⁶Departamento de Farmacia. Facultad de Ciencias de la Salud. Universidad Cardenal Herrera-CEU. Carrer Santiago Ramón y Cajal, s/n. 46113 Valencia (Spain)

⁷Instituto Universitario de Farmacia Industrial. Facultad de Farmacia. Universidad Complutense de Madrid. Plaza de Ramón y Cajal, s/n. 28040 Madrid (Spain)

⁸CRUK Formulation Unit. School of Pharmacy and Biomedical Sciences. University of Strathclyde. John Arbuthnot Building, Robertson Wing, 161 Cathedral St. Glasgow G4 0RE (United Kingdom)

⁹Departamento de Microbiología y Parasitología. Facultad de Farmacia. Universidad Complutense de Madrid. Plaza de Ramón y Cajal, s/n. 28040 Madrid (Spain)

*Corresponding author:

Dolores R. Serrano

Departamento de Farmacia Galénica y Tecnología Alimentaria

Facultad de Farmacia

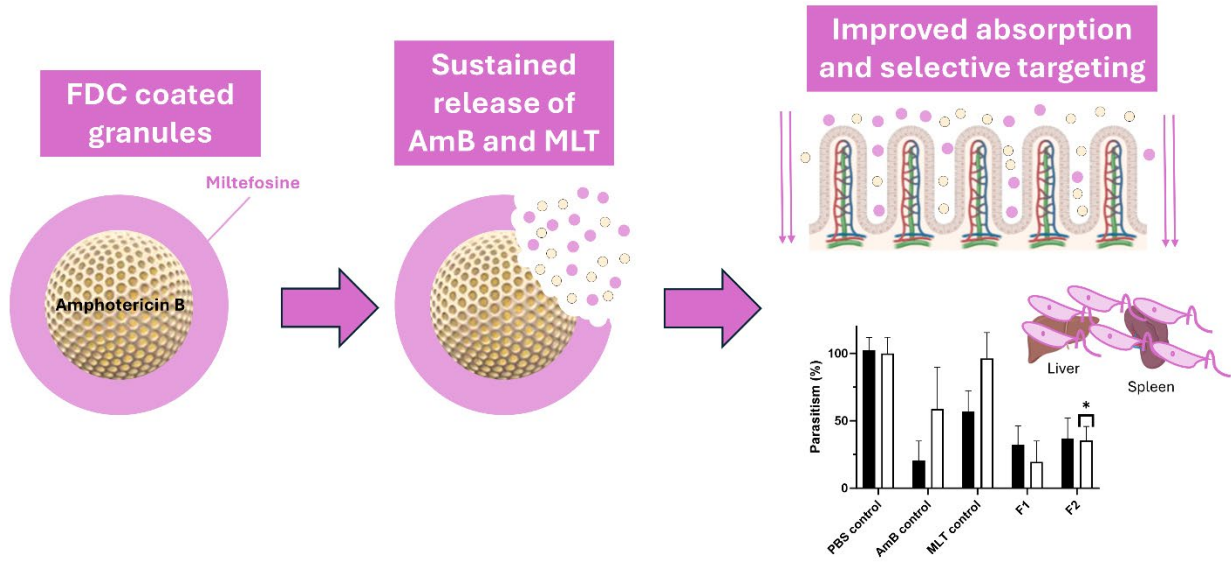
Universidad Complutense de Madrid

Plaza Ramón y Cajal, s/n

28040-Madrid, Spain

Email: drserran@ucm.es

GRAPHICAL ABSTRACT



ABSTRACT

The incidence of visceral leishmaniasis (VL) remains a significant health threat in endemic countries. Fixed-dose combination (FDC) of amphotericin B (AmB) and miltefosine (MLT) is a promising strategy for treating VL, but the parenteral administration of AmB leads to severe side effects, limiting its use in clinical practice. Here, we developed novel FDC granules combining AmB in the core with a MLT coating using wet granulation followed by fluidized bed technology. The granules maintained the crystalline structure of AmB throughout manufacturing, achieving an AmB loading of ~20%. The MLT coating layer effectively sustained AmB release from 3 to 24 hours following Korsmeyer-Peppas kinetics. The formulation demonstrated remarkable stability, maintaining >90% drug content for over a year at both 4 °C and room temperature under desiccated conditions. *In vivo* efficacy studies in *L. infantum*-infected hamsters showed 65-80% reduction in parasite burden in spleen and liver respectively, suggesting potential as an oral alternative to current VL treatments. Uncoated and coated granules demonstrated comparable performance in key aspects, including *in vivo* efficacy and long-term stability.

Keywords: oral delivery; amphotericin B; fixed-dose combination; miltefosine; coating; visceral leishmaniasis

1. INTRODUCTION

Visceral leishmaniasis (VL), also referred to as kala-azar or black fever, is the most severe form of leishmaniasis¹. VL is a potentially fatal disease caused by protozoan parasites of the *Leishmania* genus, primarily *L. donovani* and *L. infantum*². These parasites target internal organs, such as the liver, spleen and bone marrow. Symptoms include fever, weight loss, fatigue, anaemia and hepatosplenomegaly². Despite control efforts reducing incidence in some areas, VL remains a significant health threat in East Africa, India, the Mediterranean basin, China, the Middle East and South America. The disease is particularly concerning in patients co-infected with the human immunodeficiency virus (HIV)³⁻⁵. To address this situation, a strategy that has been gaining attention in recent years is the co-administration of multiple drugs with different mechanisms of action. This approach offers several advantages, including reduced adverse effects due to lower required doses to achieve the same efficacy as monotherapy, increased overall efficacy and improved patient compliance, as the treatment duration is shortened⁶⁻⁹.

Fixed-dose combination (FDC) therapy has emerged as a promising approach to treating several diseases and infections, including HIV, diabetes, dyslipidaemia, hypertension and gynaecological disorders¹⁰⁻¹². For leishmaniasis, the most effective joint treatment combines parenteral amphotericin B (AmB) with oral miltefosine (MLT), showing significantly higher cure rates than monotherapy^{4,13}. However, the utilisation of this combination therapy is hampered by several factors. The poor aqueous solubility of AmB limits its oral bioavailability (0.2-0.5%), requiring intravenous administration and hospitalisation^{14,15}. Several oral AmB formulations are under development based on nanoparticles, microemulsions and cochleates, but full parasite eradication in target tissues, such as the liver and spleen, still remains a challenge^{16,17}. This poses a particular challenge in developing countries, where healthcare resources are often limited. On the other hand, MLT, while orally bioavailable, brings several concerns, including drug resistance, adverse effects, and teratogenicity¹⁸⁻²⁰. To address these issues, developing an oral FDC product for VL treatment could revolutionise clinical practice. The anti-parasitic activity of AmB stems from its ability to bind to ergosterol in plasma membranes, forming pores that lead to a leakage of ions from the cytoplasm of parasitic cells, resulting in apoptosis²¹⁻²³. MLT, however, acts as a lipid biosynthesis inhibitor^{24,25}. Formulating AmB as part of an oral FDC product could potentially enhance its overall anti-parasitic effect through complementary mechanisms of action. The pore-forming activity of AmB may facilitate increased cellular uptake of MLT, while the disruption of lipid biosynthesis caused by MLT could potentially increase membrane fluidity, enhancing the pore-forming ability of AmB. Additionally, the oral FDC formulation might improve the bioavailability of AmB, addressing one of its main limitations as a parenteral drug⁹. This strategy represents a promising approach to current treatment limitations and an opportunity to address an unmet clinical need in VL therapy.

Wet granulation is a widely used technique for producing micron-sized granules. This process enhances the physicochemical properties of powder mixtures, particularly flow characteristics and compatibility, which are crucial for tablet manufacturing²⁶. Although conceptually simple, involving the blending of drugs with excipients, wet granulation requires precise control to achieve optimal results²⁶. Granules can serve not only as an intermediate step in tablet production but also as a final dosage form²⁷. The key to successful granulation lies in achieving an optimal balance between the active pharmaceutical ingredient and the selected excipients²⁶. Through wet granulation, immediate-release dosage forms can be formulated, allowing for rapid drug release and fast onset of action following absorption in the gastrointestinal tract²⁸. After drying and hardening, the granules can undergo further processing through spray-coating in a fluidised bed system. This additional step can alter the external properties of the granules without affecting their internal structure. Coatings serve multiple purposes, including protection against chemical and physical degradation of drugs and modification of drug release profiles²⁸. FDC granules are advancing the

pharmaceutical technology field in which drugs can be either incorporated in the coating layer or the core protected from moisture and degradation⁹.

The hypothesis that drives this work relies on the use of FDC combining AmB and MLT in a single oral dosage form that could lead to a more effective and safer anti-leishmanial treatment compared to AmB-based monotherapy, while avoiding adverse effects associated with parenteral administration. The synergy of their different mechanisms of action may result in an additive effect, potentially allowing for lower doses to elicit the same pharmacological effect. In this work, an advanced oral controlled-release FDC formulation has been developed based on water-dispersible granules with an AmB-containing core and an MLT coating layer. Active excipients were carefully selected to enhance the oral bioavailability of AmB and minimise adverse effects in the gastrointestinal tract. The rationale behind this formulation lies in the poor aqueous stability in gastric acidic media of AmB and hence, granules were engineered to place AmB in the core protected by a coating layer containing MLT. Comprehensive studies were conducted to understand the physicochemical properties of the FDC formulation and *in vivo* performance to assess AmB bioavailability, efficacy and safety profiles. This approach aims to overcome the limitations of current anti-leishmanial therapies by combining the benefits of two established drugs in a novel, patient-friendly formulation.

2. MATERIALS AND METHODS

2.1 Materials

AmB was sourced from North China Pharmaceutical Huasheng Co (Hebei, China) and MLT monohydrate from Xi'an Lyphar Biotech Co., Ltd (Xian City, China). Inulin Frutafit[®] HD (average degree of polymerisation: 10) was provided by Sensus (Roosendaal, The Netherlands). Microcrystalline cellulose (MCC) Avicel[®] PH-101 was supplied from FMC Corporation (Pennsylvania, USA). Chitosan (Mw: 100 kDa) was purchased from Guinama S.L.U. (Valencia, Spain). Sodium deoxycholate (NaDC), ethanol and dichloromethane (DCM) were supplied from Sigma-Aldrich Chemie GmbH (Buchs, Switzerland). Polyvinyl caprolactam-polyvinyl acetate-polyethylene glycol graft co-polymer (Soluplus[®]) and polyvinyl pyrrolidone (PVP) Kollidon[®] 17PF (K17) was a gift from BASF SE (Ludwigshafen, Germany). Sodium salts (Na₂HPO₄ and NaH₂PO₄, analytical grade) were purchased from Panreac Química S.A.U. (Barcelona, Spain). A nonionic poly-oxyethylene-poly-oxypropylene block co-polymer (Poloxamer 188, Pluronic[®] F68) was purchased from Thermo Fisher Scientific Inc. (Massachusetts, USA). Hydroxypropyl methylcellulose-acetate succinate (HPMC-AS, pharmaceutical grade) Aqoat[®] AS-HG was donated by Shin-Etsu Chemical Co., Ltd (Tokyo, Japan). Solvents of HPLC grade were used. All other chemicals were of reagent grade and were used without further purification.

2.2 Methods

2.2.1 Preparation of AmB-MLT FDC granules

FDC granules were prepared using a two-step process of wet granulation followed by spray-coating, as previously described⁹. The composition of the granule core and theoretical amounts of each component are detailed in Table 1.

Table 1. Composition of FDC granule core. Key: amphotericin B (AmB), microcrystalline cellulose (MCC), sodium deoxycholate (NaDC).

Component	Weight percentage (%)
AmB	25.00
Inulin	17.64
MCC	19.60
Chitosan	10.00
NaDC	6.83
Soluplus [®]	13.64
Na ₂ HPO ₄	5.00
NaH ₂ PO ₄	2.25

The listed ingredients were accurately weighed and blended using a mortar and a pestle. A 2.5% w/v aqueous solution of PVP K17 was added dropwise as a binder until a solid wet mass formed. The wet mass was passed through a series of sieves (Endecotts Ltd., London, United Kingdom) (1 mm, 710 µm, 500 µm, 350 µm and 149 µm) to obtain granules of different sizes. The granules were dried overnight at room temperature, protected from light. The largest mass fraction (>500 µm) was separated for spray-coating to minimise attrition.

The spray-coating process was conducted using a Mini-Glatt[®] fluidised bed coater equipped with a Wurster insert (Glatt[®], Binzen, Germany). Coating solutions were prepared with a 1:2 MLT:excipient weight ratio. Two formulations were manufactured, using either Soluplus[®] alone or a mixture of HPMC-AS and Poloxamer 188 (2:1 w:w) as excipients. The drug-polymer mixture was dissolved in 170 mL of ethanol:DCM (1:1 v:v) with a drug concentration of 8.4 mg/mL. The coating parameters were set as follows: 40 °C inlet temperature, 0.5 mm nozzle diameter, 3.8 g/min spray rate, 25 m³/h nitrogen flow rate and 0.8 bar atomisation pressure.

2.2.2 Physicochemical characterisation of FDC-coated granules

2.2.2.1 AmB content

AmB content within the granules was determined by dispersing 10 mg of granules (n=3) in 2 mL of dimethylsulfoxide (DMSO) (Scharlab S.L., Barcelona, Spain). The resulting dispersion was filtered through 0.45 µm PTFE filters (Thermo Fisher Scientific Inc., Massachusetts, USA) and appropriately diluted with methanol for HPLC analysis. A Jasco HPLC (Jasco Co., Tokyo, Japan) was used, comprising a DG-2080-53 3-line degasser, a LG-2080-02 ternary gradient unit, a PU-1580 ternary pump, a UV-1575 intelligent UV/vis detector and a AS-2050 Plus intelligent autosampler. Chromatographic separation was achieved using a BDS Hypersil C18, 5 µm (200 x 4.6 mm) column (Thermo Fisher Scientific Inc., Massachusetts, USA). The mobile phase consisted of acetonitrile:acetic acid:water (52:4.3:43.7, v/v) filtered through a 0.45 µm Supor[®]-450 membrane filter with a diameter of 47 mm (Pall Co., Michigan, USA). An isocratic elution method was employed for elution at room temperature with a flow rate of 1 mL/min. The injection volume was 100 µL and UV detection was performed at 406 nm. Data analysis was conducted using Borwin software²⁹.

2.2.2.2 Particle size distribution (PSD)

PSD was determined using a Mastersizer 2000 (Malvern Panalytical Ltd., Malvern, United Kingdom) through laser diffraction. Measurements were performed in triplicate. The instrument was equipped with a Scirocco dry powder feeder, operating at a 1 bar pressure and a vibration feed rate of 50%. To evaluate the

thickness of the coating layers, the median particle size (D_{50}) values were obtained for both the uncoated and coated formulations. The coating thickness was then calculated using Eq. 1³⁰:

$$\text{Thickness } (\mu\text{m}) = \frac{D_{50} \text{ after coating} - D_{50} \text{ before coating}}{2} \quad (\text{Eq. 1})$$

2.2.2.3 Surface area analysis

Surface area measurements were conducted using the Brunauer-Emmett-Teller (BET) isotherm method with a Micromeritics Gemini 2385c surface area and pore size analyser (Micromeritics Instrument Corp., Georgia, USA). The BET multiple-point method was employed, using nitrogen adsorption to determine surface area. Six data points were obtained within the relative pressure (P/P_0) range of 0.05 to 0.3. Before analysis, samples were prepared by purging under nitrogen overnight at 25 °C. Each result represented the average of three measurements³¹.

2.2.2.4 Scanning electron microscopy (SEM)

The morphology of the formulations was examined using SEM. A JSM 6335F (Jeol Ltd., Tokyo, Japan) equipped with a secondary electron detector was employed, providing image resolutions of 1.5 nm at 15 kV and 5 nm at 1 kV. To visualise the surface, the coating layer and the core of the coated formulations, granules were halved using a sharp blade. The samples were then mounted on aluminium pins using carbon tabs and sputter-coated with gold prior to imaging.

2.2.2.5 Thermogravimetric analysis (TGA)

Water content was determined using TGA with a TGA Q50 measuring module (TA Instruments®, Delaware, USA). Samples were analysed in triplicate ($n=3$) using aluminium pans, with nitrogen as the purge gas. The temperature range for analysis was 50-200 °C, with a heating rate of 10 °C/min. Data analysis was performed using TA Universal Analysis® software version 4.5A (TA Instruments®, Delaware, USA).

2.2.2.6 Modulated temperature differential scanning calorimetry (DSC)

MTDSC analysis was conducted using a DSC Q200 (TA Instruments®, Delaware, USA) with nitrogen as the purge gas. Samples weighing 2-3 mg were placed in aluminium pans and analysed over a temperature range of 0-200 °C. The modulation rate was set at 0.8 °C every 60 seconds, with a scanning rate of 5 °C/min. TA Universal Analysis® software version 4.5A (TA Instruments®, Delaware, USA) was used for data processing. The instrument was calibrated using indium as a standard. Melting event temperatures ($n=3$) were reported as onset temperatures.

2.2.2.7 Fourier-transform infrared spectroscopy (FTIR)

FTIR spectroscopy analysis was performed using a Spectrum 1 FT-IR spectrometer (PerkinElmer Inc., Massachusetts, USA) equipped with a Universal Attenuated Total Reflectance (UATR) accessory and ZnSe crystal. Spectra were collected in sextuplicate ($n=6$) over the range of 600-4000 cm^{-1} . Data normalisation was conducted using Spectragryph® software version 1.2.9 (The Spectroscopy Ninja®, Berchtesgaden, Germany).

2.2.2.8 Powder X-ray diffraction (PXRD)

PXRD analysis was performed in triplicate using a Miniflex II diffractometer (Rigaku Co., Tokyo, Japan). The instrument employed Ni-filter $\text{Cu K}\alpha$ radiation with a wavelength of 1.54 Å. Operating conditions were

set at 30 kV tube voltage and 15 mA tube current. PXRD patterns were recorded over a 2θ ranging from 5° to 40° at a step scan rate of 0.05° .

2.2.2.9 Dynamic vapour sorption (DVS)

Vapour sorption experiments were conducted using a DVS Advantage-1 automated gravimetric sorption analyser (Surface Measurement Systems Ltd., London, United Kingdom) at $25 \pm 0.1^\circ\text{C}$, with water as the probe vapour. Samples (15-20 mg) were initially dried at 0% relative humidity (RH) for 1 hour. The RH was then cycled from 10% to 90% for sorption and reversed for desorption. The RH was changed only after the sample mass reached equilibrium, defined as $dm/dt \leq 0.002$ mg/min over 10 minutes. Two complete sorption-desorption cycles were recorded for each sample³². Following DVS analysis, samples were evaluated by PXRD.

2.2.3 Dissolution profile of AmB

Dissolution studies were conducted using simulated gastric fluid (SGF) and simulated intestinal fluid (SIF). SGF (500 mL) without enzymes was prepared using HCl and deionised water, adjusting the pH to 1.2³³. An Erweka DT80 dissolution apparatus (Erweka GmbH, Hessen, Germany) was used, while the medium was heated to 37°C for 1 hour to simulate physiological temperature. Granules (25 mg) were added to each vessel and dissolution was performed using paddles at 100 rpm under sink conditions in two steps. First, SGF was used for 30 minutes, followed by the addition of 400 mL of SIF supplemented with 0.5% (w/v) sodium dodecyl sulphate (Thermo Fisher Scientific, Massachusetts; USA) to ensure AmB dissolution under sink conditions. The pH was then adjusted to 6.8 using 2.5 mL of a 30% (w/v) NaOH solution. Samples (5 mL) were withdrawn without media replacement at several time points (5, 10, 15, 30, 45, 60, 90, 120, 150, 180, 240, 360 and 1440 minutes), centrifuged at 5000 rpm for 5 minutes and the supernatant was analysed using the previously described HPLC method. All dissolution media were prepared according to Pharmacopoeia standards and studies were performed in triplicate³³. The dissolution profile was fitted to different release kinetics models, including zero order (constant dissolution regardless of concentration), first order (release depending on concentration), Higuchi (for drug release from an insoluble matrix based on Fickian diffusion), Korsmeyer-Peppas (for polymeric systems with multiple release mechanisms simultaneously) and Hixson-Crowell (for formulations with uniform particle size)³⁴⁻³⁶. The dissolution profile of MLT was not evaluated considering its high aqueous solubility (≥ 2.5 mg/mL)²⁵.

2.2.4 Accelerated predictive stability studies (APS)

Prior to accelerated stability testing, all formulations were stored in a desiccator containing silica gel at $4 \pm 1.21^\circ\text{C}$ and $11.01 \pm 1.64\%$ RH. The Cuspor Ageing System™ was employed for ageing each formulation. Humidity capsules were placed in Cuspor chambers and pre-equilibrated at the selected temperature to ensure stable RH conditions before introducing the samples³⁷. Approximately, 5 mg of each sample were weighed into uncapped HPLC vials and placed in the stability chambers. Granules were exposed to various temperature and RH conditions: $50^\circ\text{C}/10\%$ RH, $50^\circ\text{C}/50\%$ RH, $60^\circ\text{C}/75\%$ RH, $70^\circ\text{C}/10\%$ RH and $70^\circ\text{C}/50\%$ RH (Table 2). At predetermined time points, samples were collected, dissolved in DMSO, further diluted with mobile phase and analysed using the previously described HPLC method.

Table 2. APS time points and storage conditions of granules.

Time (days)	Temperature (°C)	RH (%)
1	60	75
	70	10
		50
2	60	75
3	50	50
		10
	70	50
5	60	75
7	50	10
		50
	60	75
		10
	70	50
10	70	10
		50
14	50	10
		50
21	50	10

Stability modelling was conducted to analyse the degradation kinetics of AmB. The degradation data were fitted to various models, including zero order, first order, second order, Avrami and diffusion models. To comprehensively understand the combined effects of temperature and RH on AmB, a humidity-corrected Arrhenius equation was used (Eq. 2)^{38,39}:

$$\ln K = \ln A - \frac{E_a}{RT} + B(RH) \quad (\text{Eq. 2})$$

where K was the degradation constant, A was the collision frequency, E_a was the activation energy, R was the gas constant, T was the absolute temperature, B was the humidity sensitivity factor and RH was the relative humidity. The B term was calculated using the following equation (Eq. 3):

$$B(RH) = \frac{\ln\left(\frac{k_1}{k_2}\right)}{RH_1 - RH_2} \quad (\text{Eq. 3})$$

where k_1 and k_2 were the degradation constants calculated at the same temperature but different relative humidities, RH_1 and RH_2 , respectively. An averaged B term calculated at the different temperatures was used. Long-term stability studies were performed at 25 °C/10 % RH and 4 °C/10 % RH.

2.2.5 *In vitro* anti-parasitic activity

Granules were also evaluated in terms of anti-parasitic activity against *L. donovani* and *L. infantum* according to previously described protocols^{40,41}. The experiment was carried out in promastigote forms of *Leishmania*. Parasites were cultured in Schneider's insect medium (Merck KGaA, Darmstadt, Germany) at 26 °C and supplemented with heat-inactivated foetal bovine serum (FBS) (Merck KGaA, Darmstadt, Germany), penicillin and streptomycin at a concentration of 100 IU/mL and 100 µg/mL, respectively. Briefly, late log-phase promastigotes were cultured in 96-well plates and 2.5×10^6 parasites were added per well. Formulations were diluted in de-ionised water up to a AmB concentration of 1 mg/mL. All samples were added in triplicate. After 48 hours of incubation at 26 °C, a resazurin solution (20 µL, 2.5 mM) was added to each well and, 3 hours later, the fluorescence intensity (535 nm excitation wavelength, 590

emission wavelength) was measured using a Tecan® Infinite 200 fluorimeter (Tecan Group Ltd., Männedorf, Switzerland). Data analysis was performed using GraphPad Prism software version 7.02 (GraphPad Software Inc., California, USA) to calculate growth inhibition. The efficacy of each formulation was expressed as the IC₅₀ (concentration needed to inhibit growth in 50% of the parasites)³³.

2.2.6 *In vitro* cytotoxicity in J774 macrophages

J774 macrophages were cultured in RPMI-1640 medium supplemented with FBS, penicillin (100 IU/mL) and streptomycin (100 µg/mL). Cells were then maintained at 37 °C in a humidified environment (5% CO₂). Macrophages were placed in 96-well plates (5 x 10⁴ cells/well) with 100 µL of RPMI-1640 medium and incubated for 24 hours at 30 °C, 5% CO₂. Later, the medium was discarded; replaced with 200 µL of formulation and incubated again for 24 hours. After that, resazurin (20 µL, 1 mM) was added and the plates were incubated for another 3 h. Then, absorbance was measured at 590 and 595 nm. All samples and controls (drugs dissolved in DMSO) were tested in triplicate. The safety of each formulation was assessed by the calculation of the CC₅₀ (concentration needed to produce cytotoxicity in 50% of macrophages). Selectivity index (SI) was used to evaluate the relative toxicity to healthy macrophages compared to the efficacy against *Leishmania*. SI was calculated as follows (Eq. 4):

$$SI = \frac{CC_{50}}{IC_{50}} \quad (\text{Eq. 4})$$

where CC₅₀ was the concentration needed to produce cytotoxicity in 50% of healthy macrophages and IC₅₀ was the concentration needed to inhibit growth in 50% of parasites³³.

2.2.7 *Ex vivo* haemolysis in red blood cells (RBCs)

The haemolytic toxicity assay was conducted using a modified version of a previously described method^{42, 43}. Blood was collected from a healthy human donor in lithium-heparin-coated Vacutainer™ tubes (Becton, Dickinson and Co., New Jersey, USA) to prevent coagulation. The blood was then centrifuged at 1,000 g for 5 minutes to separate the RBCs from the plasma. After removing the plasma, the RBCs were washed multiple times with a 150 mM NaCl solution, with centrifugation repeated between washes. The washed RBCs were then diluted to a 4% (v/v) concentration using phosphate buffer (pH 7.4).

For the assay, granule dispersions were prepared in water at AmB concentrations ranging from 0.78 to 100 µg/mL. These dispersions were combined with the diluted RBCs in a 1:1 v:v ratio in 96-well plates, with all tests performed in triplicate. Positive control wells containing 20% Triton® X-100 (Merck KGaA, Darmstadt, Germany) and negative control wells with PBS (pH 7.4) were included. The plates were incubated at 37 °C for 1 hour using an orbital rocker, then centrifuged at 500 g for 5 minutes to pellet intact RBCs. The supernatant was transferred to a new clear plate and the absorbance was measured at 570 nm using a BioTek ELx808 UV-plate reader (BioTek Instruments Inc., Vermont, USA) to quantify released haemoglobin, indicating cell lysis.

The haemolytic toxicity was then calculated using the following equation (Eq. 5):

$$\text{Haemolysis (\%)} = \frac{ABS(\text{sample}) - ABS(\text{PBS})}{ABS(\text{Triton X})} \times 100 \quad (\text{Eq. 5})$$

2.2.8 *In vivo* efficacy studies against *Leishmania*

L. infantum parasites (MHOM/BR/72/46 strain) were grown in M199 medium (Sigma-Aldrich, Darmstadt, Germany) supplemented with 10% foetal calf serum (FCS), 50,000 IU/mL penicillin, 50 µg/mL streptomycin, at 25 °C. Stationary phase promastigotes were used throughout the entire study.

Female golden hamsters (*Mesocricetus auratus*) (8-week-old) were obtained from the Medical School of the University of São Paulo, Brazil. This study was carried out in strict accordance with the recommendations detailed in the Guide for the Care and Use of Laboratory Animals of the Brazilian National Council of Animal Experimentation (<http://www.cobea.org.br>). The protocol was approved by the Ethics Committee of Animal Experiments of the Institutional Committee of Animal Care and Use at the Medical School of São Paulo University (Number 056/16 and 344A). For all experimental procedures, the animals were anaesthetised with thiopental (1 mg/200 µL).

Twenty-five animals were intraperitoneally infected with 2×10^7 promastigote forms of *L. infantum*. Sixty days after infection, *L. infantum* infected hamsters were divided into five groups: group 1 (n=5) was orally treated with the formulation consisting of the uncoated AmB core (F1), group 2 (n=5) was orally treated with the combined formulation consisting of AmB and MLT (F2), group 3 (n=5) was intraperitoneally treated with AmB-deoxycholate (AmB control), group 4 (n=5) was orally treated with MLT (MLT control) and group 5 (n=5) was orally treated with vehicle solution (PBS control)^{44,45}. F1 and F2 were administered after being previously dispersed in water to achieve an AmB concentration of 1 mg/mL. All treatments were administered daily (at a fixed AmB dose of 5 mg/kg and a MLT dose of 2.33 mg/kg), once a day over the course of 7 consecutive days. Animals were weighted before and after the 7-day treatment to monitor any variations in weight that could indicate gastrointestinal toxicity. Weight differences were calculated as follows (Eq. 6):

$$\text{Weight difference (g)} = \text{Weight after treatment (g)} - \text{Weight before treatment (g)}$$

Seven days after the last dose, animals were sacrificed in a CO₂ chamber and the spleen and liver were collected to quantify tissue parasitism by limiting-dilution assay⁴⁶.

Briefly, fragments of the spleen and liver from the different groups were aseptically collected, weighed and homogenised in M199 medium. The suspensions of organs were subjected to 12 serial dilutions with four replicate wells. The number of viable parasites was determined based on the highest dilution rate where promastigote forms could be observed after 15 days of cultivation at 25 °C.

2.2.9 Statistical analysis

Minitab[®] 16 (Minitab Inc., Coventry, United Kingdom) was utilised to perform one-way ANOVA. Tukey's test was used to establish a comparison among formulations and find statistically significant differences between groups. P-value < 0.05 between groups was considered a statistically significant difference.

3. RESULTS

3.1 Physicochemical characterisation of AmB-MLT granules

3.1.1 AmB content

The AmB content in the uncoated granules was $21.05 \pm 1.43\%$ (Table 3). Following the coating process, a reduction in AmB loading was observed, with values around 18%, which was attributed to the dilution effect resulting from the addition of the coating layer, which increased the overall mass of the granules without contributing additional AmB.

Table 3. Physicochemical properties of coated granules (n=3). Key: Statistically significant differences between F1 and the other two formulations were represented by * ($p < 0.05$, one-way ANOVA post-hoc test).

3.1.2 Particle size distribution (PSD), surface area and morphology

The D_{50} of uncoated granules was $674 \pm 12 \mu\text{m}$. After coating, the radius of the granules increased by approximately $200 \mu\text{m}$ when using Soluplus[®] and by about $115 \mu\text{m}$ with HPMC-AS and Poloxamer 188. These values represented the thickness of the coating layer (Table 2). Conversely, the surface area decreased 2-4-fold from uncoated to coated granules as the coating layer acted as a sealing protective layer (Table 2) which was aligned with the reduction in water content from $\sim 8\%$ to below 4% (Table 2) in the coated granules.

SEM micrographs revealed that uncoated granules were quasi-spherical, ranging from 500 to $800 \mu\text{m}$ in size (Fig. 1a-b). Their surface comprised multiple small crystals ($1-20 \mu\text{m}$), explaining their greater surface area. In contrast, coated formulations showed a smoother surface (Fig. 1c-f). Cross-sectional images of halved granules showed the porous core structure and the thickness of the coating layer (Fig. 1d and 1f).

Formulation	Drug in the core	Composition (binding agent)	Drug in the coating layer	AmB content (%)	Water content (%)	D_{50} (μm)	Thickness of coating layer (μm)	Surface area (m^2/g)
F1	AmB	-	-	21.05 ± 1.43	7.95 ± 0.03	674.0 ± 11.9	-	2.511 ± 0.008
F2	AmB	Soluplus [®]	MLT	$18.04 \pm 1.73^*$	3.48 ± 0.03	1091.5 ± 5.6	208.75 ± 8.75	1.140 ± 0.007
F3	AmB	HPMC-AS Poloxamer 188	MLT	$18.21 \pm 1.81^*$	2.34 ± 0.04	903.6 ± 7.5	114.8 ± 9.70	0.564 ± 0.002

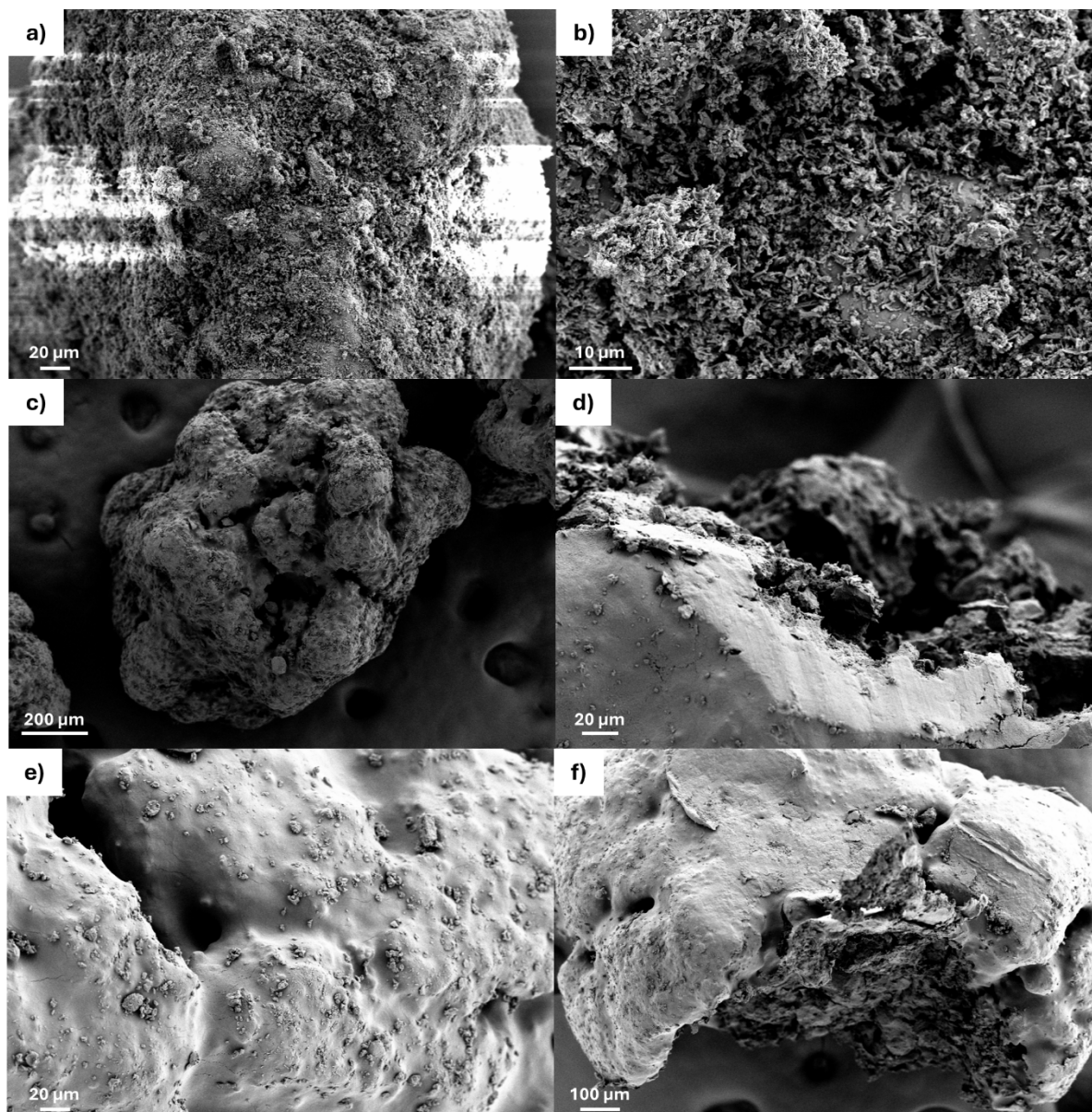


Figure 1. SEM micrographs of F1 (a, b), F2 (c, d) and F3 (e, f) showing the morphology of the core and the coating layer of each formulation.

3.1.3 Modulated temperature-differential scanning calorimetry (MT-DSC)

DSC thermogram of AmB shows a notable broad endotherm at 148.1 °C, which is consistent with literature reports of the thermal behaviour of AmB, possibly indicating melting followed by degradation (Fig. 2a). DSC thermogram of MLT monohydrate shows a dehydration endotherm with an onset temperature of 89.9 °C which matches with previous reports⁴⁷. The subtle event at 51.9 °C is attributed to a solid-solid transition or the melting of a minor impurity (Fig. 2a). The melting event of MLT was not recorded as occurs at higher temperatures being described as melt-decomposition endotherm with onset at 265.4 °C⁴⁷. The formulations demonstrated similar thermal profiles to individual components but with lower heat flows which were attributed to the dilution factor with the excipients as well as the amorphisation occurring during the spray-coating process.

3.1.4 Fourier-transform infrared spectroscopy (FTIR)

The FTIR spectral analysis of AmB exhibited a broad peak between 3481 and 3294 cm^{-1} , indicative of O-H or N-H stretching, along with a weak, but characteristic peak at 1556 cm^{-1} , likely due to C=C stretching in the conjugated double bonds in the hydrophilic chain of AmB. In contrast, MLT displayed a sharp C-H stretching peak at 2914 cm^{-1} (Fig. 2b). F1 retained similarities to the AmB spectrum, with some modifications in peak intensities, but no shift in the characteristic peak at 1556 cm^{-1} . Coated formulations both demonstrated a merger of AmB and MLT spectral features, with subtle differences in the fingerprint 1500-1000 cm^{-1} region (Fig. 2b). Interestingly, the AmB peak at 1556 cm^{-1} disappeared for both F2 and F3, likely due to the interaction between AmB and the coating materials. To sum up, all formulations exhibited some degree of peak broadening and intensity changes compared to the raw materials.

3.1.5 Powder X-ray diffraction (PXRD)

AmB exhibited characteristic Bragg peaks at 14.3° and 21.9° 2θ , which were also present in the uncoated granules. This indicated that AmB maintained its crystalline form after granulation. The diffraction pattern of coated granules for these peaks closely resembled those of uncoated AmB granules, but with sharper peaks, suggesting that AmB remained crystalline after spray-coating with an apparent reorganisation of the crystals into a more ordered arrangement⁴⁸ (Fig. 2c). MLT, on the other hand, displayed distinct Bragg peaks at 7.1°, 14.5°, 17.7° and 21.9° 2θ . However, in the F3 formulation coated with HPMCAS/Poloxamer 188, only AmB-associated Bragg peaks were observed (Fig. 2c). The absence of MLT peaks in this formulation suggested that MLT transitioned to an amorphous state during the coating process.

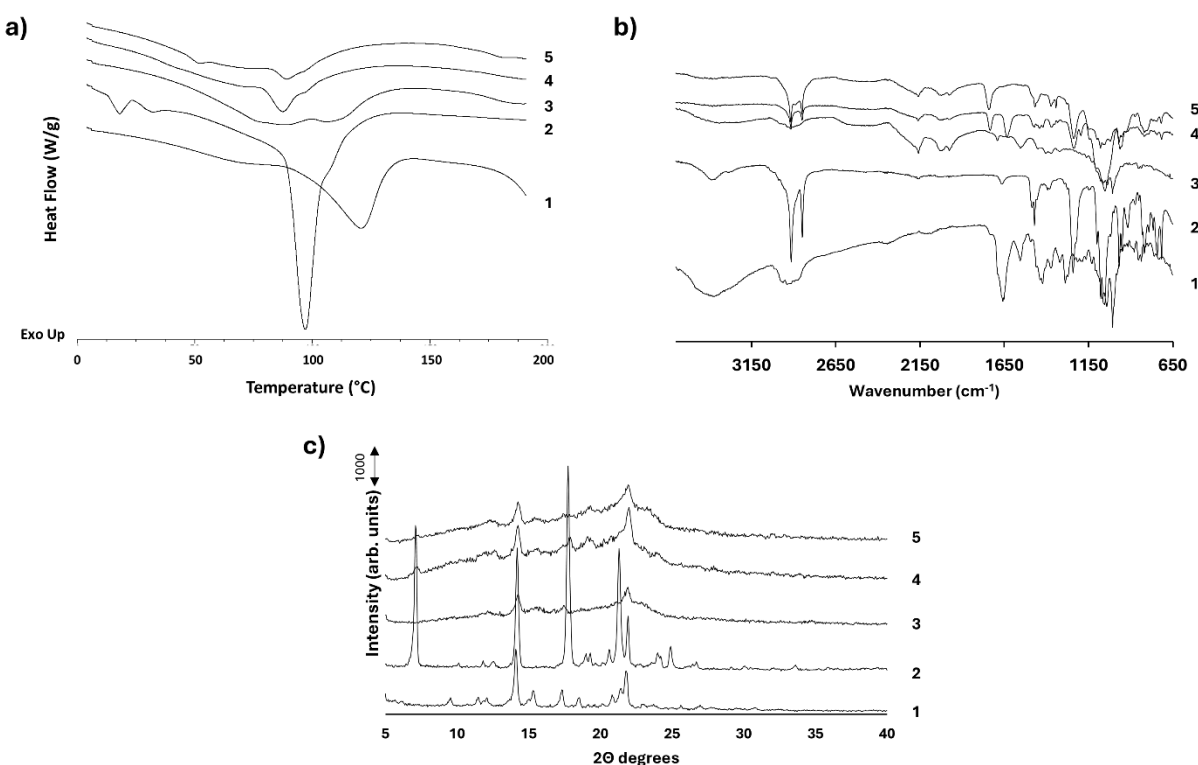


Figure 2. Physicochemical characterisation of FDC granules: a) DSC thermograms; b) FTIR spectra; c) PXRD patterns. Key: AmB raw material (1), MLT raw material (2), F1 (3), F2 (4) and F3 (5).

3.1.6 Dynamic vapour sorption (DVS)

DVS analysis revealed distinct moisture uptake patterns for uncoated and coated granules (Fig. 3a). The uncoated formulation (F1) exhibited the highest water uptake, reaching approximately 20% at 90% RH, displaying more pronounced hysteresis. In contrast, the coated formulations F2 and F3 showed a lower water uptake, with maximum values of 17.5% and 14.8%, respectively. Notably, all formulations maintained consistent mass across two sorption-desorption cycles, indicating stability against recrystallisation. This stability was further corroborated by PXRD analyses conducted post-DVS, which revealed no alterations in the diffraction patterns of any formulation (Fig. 3b).

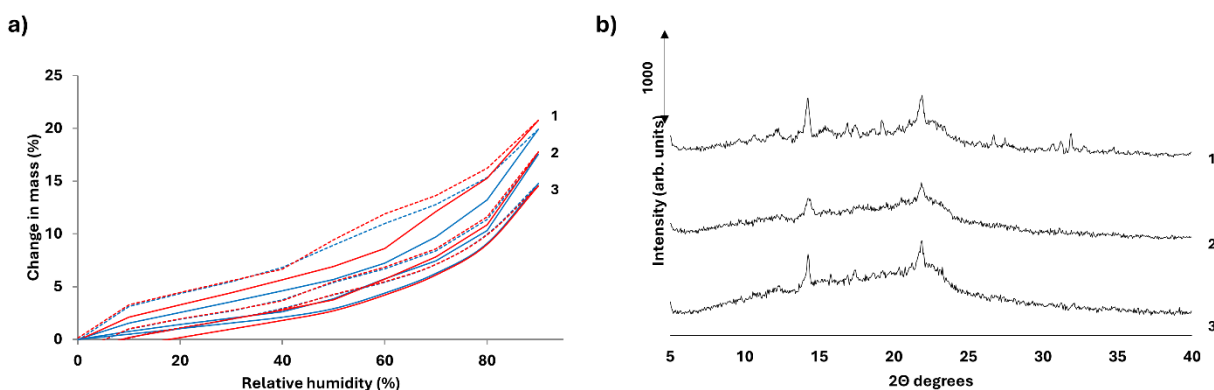


Figure 3. DVS sorption (solid lines) and desorption (dash lines) isotherms of first (blue lines) and second cycles (red lines) (a) and post-DVS PXRD analyses (b). Key: F1 (1), F2 (2) and F3 (3).

3.2 Dissolution studies

Figure 4 illustrates the dissolution profiles of AmB across the three formulations. The uncoated AmB core (F1) demonstrated pH-dependent release kinetics. At pH 1.2, less than 1% of AmB was released within the first 30 minutes. However, upon increasing the pH to 6.8 a rapid release was triggered, resulting in a complete dissolution after 180 minutes. Dissolution data modelling revealed that F1 followed Korsmeyer-Peppas kinetics with Fickian diffusion (release exponent, $n < 0.43$) (Table 4). Notably, the granules maintained their structural integrity for 2-3 hours during the dissolution study, while their density allow them to float for the whole duration of the experiment. The polymer coating in formulations F2 and F3 played a critical role in modulating the release of AmB. The coating materials (Soluplus[®] in F2 and HPMC-AS/Poloxamer 188 in F3) served as diffusion barriers, as these formulations exhibited significantly slower dissolution rates compared to F1 and exhibited approximately 50% release rate after 24 hours (Fig. 4). Both coated formulations also followed Korsmeyer-Peppas kinetics, but with distinct mechanisms: F2 displayed Fickian diffusion ($n < 0.43$), while F3 showed an anomalous mechanism combining diffusion and erosion ($0.43 < n < 0.85$) (Table 4).

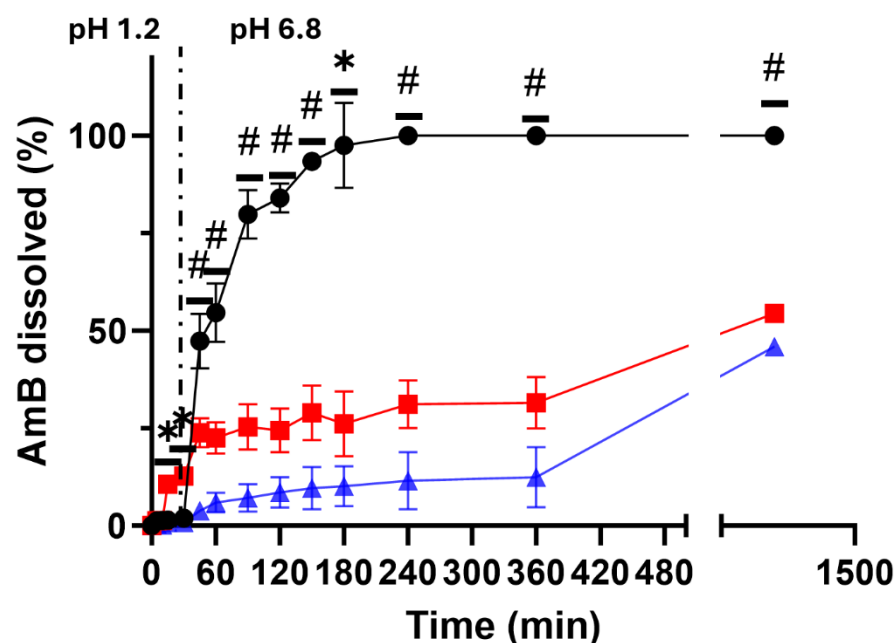


Figure 4. Cumulative drug release profile for AmB. Key: F1 (black circles), F2 (red squares) and F3 (blue triangles). Statistically significant differences between F1 and the other two formulations were represented by *, while # showed statistically significant differences among the three formulations ($p < 0.05$, one-way ANOVA post-hoc test).

Table 4. Drug release kinetics from FDC coated granules.

Formulation	Zero order (R^2)	First order (R^2)	Higuchi (R^2)	Korsmeyer-Peppas (R^2)	Hixson-Crowell (R^2)
F1	0.8808	0.9658	0.9698	0.9958 ($n=0.2940$)	0.9546
F2	0.6667	0.7305	0.8098	0.9763 ($n=0.279$)	0.7083
F3	0.9680	0.9671	0.9091	0.9724 ($n=0.821$)	0.9685

3.5 Accelerated predictive stability studies (APS)

Formulations F1 and F2 were evaluated for long-term stability and APS. F3 was discarded bearing in mind the slow-release kinetics in physiological media. Long-term stability studies revealed that all formulations maintained chemical stability for at least one year under refrigerated conditions and at room temperature in desiccated environments, with drug content remaining above 90%. Humidity significantly impacted the chemical stability of AmB in the uncoated formulation (F1), as evidenced by a greater B term of 0.007. In contrast, F2 showed no susceptibility to humidity, suggesting that its coating effectively shielded AmB from moisture. Table 5 presents the degradation kinetics and activation energies for AmB, which followed a second order kinetic model in both formulations.

The prediction models closely aligned with the long-term experimental results, demonstrating good overall chemical stability for the formulations when stored under refrigerated or room temperature desiccated conditions for a year.

Table 5. Degradation models of AmB at the tested conditions of temperature and RH. Key: E_a (activation energy); B term (moisture sensitive factor).

Formulation	Best fitting model	E_a (kcal/mol)	B term	Predicted stability at 4 °C and 10% RH (years)	Experimental drug content after 1 year at 4 °C and 10% RH (%)	Experimental drug content after 1 year at 25 °C and 10% RH (%)
F1	Second order	15.049 ± 7.213	0.007 ± 0.002	0.977 ± 0.039	93.607 ± 1.312	91.153 ± 0.464
F2	Second order	19.146 ± 3.644	0.000 ± 0.000	1.144 ± 0.039	94.187 ± 1.653	91.793 ± 1.666

3.6 Anti-leishmanial activity and cytotoxicity of FDC granules

The *in vitro* anti-leishmanial activity of FDC granules is illustrated in Table 5. *L. donovani* and *L. infantum* were selected as these parasites are the aetiological agents responsible for VL. All FDC formulations exhibited a greater activity (3-9-fold) against *L. infantum* over *L. donovani*. Notably, uncoated AmB granules were the most active formulation against both *Leishmania* species, while dual drug-coated formulations exhibited higher values of IC_{50} , which align were the results from AmB dissolution. This can be attributed to the slower drug release from coated granules compared with the uncoated AmB formulation. AmB-DMSO controls were still more active than any of the three tested formulations.

Regarding toxicity, it was observed that FDC formulations assayed on J774 macrophages and RBCs exhibited a safer profile (selectivity index >10) than AmB dissolved in DMSO, specially formulations F1 and F3 for macrophages as well as F1 and F2 for RBCs (Table 6). F1 demonstrated the most favourable efficacy/safety balance among the formulations, as evidenced by its SI values. For *L. donovani*, the SI value was 148.15 ± 1.35 , while for *L. infantum*, it reached 444.44 ± 4.51 . These calculations were based on the maximum tested concentration of 200 µg/mL. Notably, F1 showed no cytotoxicity for macrophages at this concentration, suggesting that the actual SI values are even higher than reported in table 6.

Table 6. *In vitro* efficacy and toxicity of FDC granules. Key: IC_{50} (concentration needed to inhibit growth in 50% of parasites), SI (selectivity index), * (SI calculated at 200 µg/mL), CC_{50} (concentration needed to produce cytotoxicity in 50% of healthy macrophages), N/A (F1 did not exhibit any cytotoxicity at the highest tested concentration of 200 µg/mL), HC_{50} (concentration needed to produce haemolysis in 50% of RBCs).

Formulation	AmB-DMSO	F1	F2	F3	
<i>L. donovani</i>	IC_{50} (µM)	0.23 ± 0.01	1.35 ± 0.15	4.65 ± 0.19	4.59 ± 0.20
	SI	51.48 ± 10.09	≥148.15 ± 1.35*	3.20 ± 2.38	17.94 ± 2.49
<i>L. infantum</i>	IC_{50} (µM)	0.09 ± 0.01	0.45 ± 0.10	1.16 ± 1.26	0.48 ± 0.05
	SI	131.56 ± 20.18	≥444.44 ± 4.51*	12.85 ± 2.35	171.50 ± 2.41
CC_{50} (µM)	11.84 ± 4.03	N/A	14.91 ± 4.57	82.32 ± 4.77	
HC_{50} (µM)	37.14 ± 2.81	25.61 ± 10.15	43.17 ± 0.10	7.23 ± 1.18	

3.8 *In vivo* efficacy studies against leishmaniasis

F1 (uncoated AmB granules) and F2 (coated AmB granules) were administered orally *in vivo* in golden hamsters infected with *L. infantum* at a fixed dose of 5 mg/kg, once a day over 7 consecutive days. The

same dose regime was followed to intraperitoneally administer an AmB control and orally administer both a MLT and PBS control. The parasite burden in the liver was reduced by 41, 81 and 65% after the administration of AmB control, F1 and F2, respectively, while in the spleen it was reduced by ~65% for both tested formulations and by 79% for the AmB control. However, the animals treated with oral MLT only showed a significant decrease in parasite load in spleen (43%) (Fig. 5a).

In addition, animals gained weight during the whole treatment, indicating good gastrointestinal tolerance and absence of acute gastrointestinal toxicity (Fig. 5b)⁴⁹.

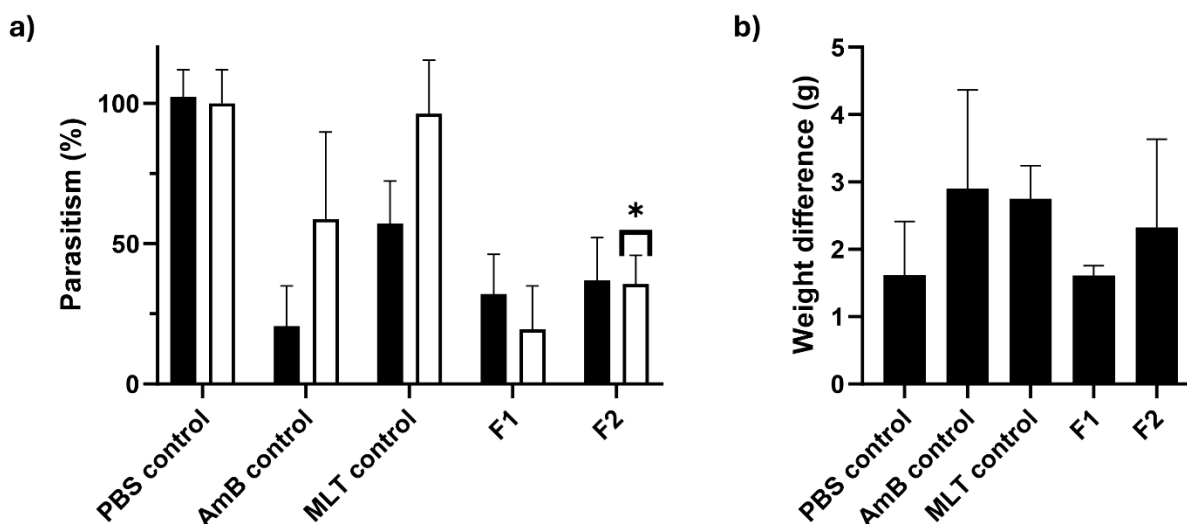


Figure 5. *In vivo* evaluation of FDC granules in *L. infantum* infected golden hamsters: **a)** Cumulative parasite burden (*L. infantum*) in the spleen (black) and liver (white) after a once-daily 7-day treatment course with AmB control (5 mg/kg), MLT control (2.33 mg/kg) F1 (5 mg/kg) and F2 (5 mg AmB/kg and 2.33 mg MLT/kg); **b)** Body weight change in golden hamster before and after the 7-day treatment course. Statistically significant difference between the formulation groups and the MLT control group is represented by * ($p < 0.05$, one-way ANOVA post-hoc test). No significant difference was observed between the formulation groups and the AmB control.

4. DISCUSSION

The development of oral therapies for the treatment of VL remains challenging due to the poor aqueous solubility of most anti-leishmanial drugs. To the best of our knowledge, this is the first report of an orally fixed-dose formulation combining AmB with MLT. In this work, the *in vitro* and *in vivo* performance of uncoated and coated AmB-MLT granules was explored to understand the impact of a coating sealing layer on AmB granules to protect them from moisture. The morphology of the granules was significantly transformed after coating from a rough to a smooth surface. The sealing effect was corroborated by DVS studies indicating a lower hygroscopicity of coated granules which was aligned with greater chemical stability but resulted in a detriment in the release kinetics that impacted the final *in vivo* performance.

Drug release studies provided valuable insights into the behaviour of the formulations. F1 demonstrated the fastest AmB release with a pH-dependent dissolution profile, with minimal release occurring in acidic conditions. This characteristic is particularly advantageous, as it could prevent premature drug release in the acidic environment of the stomach where AmB degrades faster, instead favouring release in the intestine, where absorption is more efficient. The coated formulations, F2 and F3, exhibited slower AmB release rates due to the barrier effect of the coating layer. All formulations followed Korsmeyer-Peppas

release kinetics, though with varying mechanisms depending on their composition. While F1 and F2 fitted to a Fickian diffusion ($n < 0.43$), F3 showed an anomalous mechanism combining diffusion and erosion ($0.43 < n < 0.85$). The latter is usual in oral formulations containing cellulose derivatives, such as HPMC, so it could be attributed to the polymers employed for coating, while Fickian diffusion could be explained by the quasi-spherical shape of the granules, which was maintained during the dissolution study for at least 2 hours. As the shape of the granules influences the surface area exposed to the dissolution medium and how the drug molecules move out of the matrix, a quasi-spherical shape has a relatively constant surface area during dissolution, meaning that the rate at which the drug is released remains steady over time⁵⁰. Nevertheless, MLT release was not studied due to its high aqueous solubility (≥ 2.5 mg/mL) and the lack of strong chromophores in its chemical structure, which makes ultraviolet and fluorescence detection very difficult⁵¹.

Stability studies demonstrated that all formulations remained chemically stable for at least one year when refrigerated and at room temperature under desiccated conditions. RH played a crucial role in AmB stability, particularly affecting F1 due to the lack of a protective coating layer. The coating in F2 served as an effective moisture barrier, enhancing its stability. In both F1 and F2, AmB degradation followed second order kinetics. This suggests that the degradation process is more complex and the degradation rate does not depend linearly on concentration. A second order model implies that interactions between AmB molecules, between AmB and MLT or between AmB and excipients may play a significant role in the degradation process, rather than the sole influence of the concentration of AmB⁵². The coating layer did not modify the degradation kinetics of AmB, unlike in the previously developed formulation containing AmB in the core and itraconazole in the coating layer, in which AmB followed an Avrami degradation model⁹.

The combination of miltefosine alongside intravenous liposomal amphotericin B in HIV-coinfected VL patients in East Africa significantly improved cure rates and reduced failure rates for both primary VL and VL relapse compared to high-dose AmBisome monotherapy⁵³. This shows the immense potential for combining AmB and MLT within the same oral solid dosage form to facilitate regimens and enhance patient compliance and clinical performance. To maintain the physicochemical compatibility between both drugs, they were contained in different sections of the granules, AmB in the core and MLT in the coating layer minimizing physicochemical interactions.

The formulations showed significant *in vitro* anti-parasitic activity against both *L. donovani* and *L. infantum*, with F1 demonstrating the highest efficacy, which is aligned with its fastest release. Based on their *in vitro* performance, the F1 (uncoated AmB granules) and F2 (coated AmB-MLT with Soluplus®) were selected for further *in vivo* testing, revealing that both formulations significantly reduced the presence of *L. infantum* parasites in the spleen and liver of golden hamsters compared to the control group. This indicated drug accumulation in both tissues to elicit the pharmacological effect observed. The combination of AmB and MLT did not result in higher efficacy compared to the uncoated granules which can be attributed to the partial release of AmB from the core. However, we hypothesise that upon dissolution in the gastrointestinal tract, MLT could enhance AmB solubilisation triggering into micelles and promoting absorption through the Peyer's patches. Serrano et al. showed that AmB encapsulation in modified chitosan nanoparticles significantly enhanced oral bioavailability by up to 24% through the gut-associated lymphoid tissue via the lymphatic vessels to the systemic circulation, which explains the drug accumulation in the spleen and the liver¹⁷. Additionally, the increase in body weight is an encouraging insight into the overall tolerability of these FDC formulations which is related to optimal gastrointestinal tolerability, although toxicity studies should be carried out to assess the safety of the formulation and to confirm that the increase in body weight is not related to ascites due to liver failure.

Even though the coating layer protected AmB from degradation, further development should aim for a faster release at the intestinal pH to enhance oral bioavailability and then, *in vivo* efficacy, as the slow release of AmB might cause a lack of absorption of the drug before being excreted. Formulating both drugs

in the core could be advantageous to increase the MLT dose in the formulation and also to diminish the thickness of the coating layer to ensure a faster release. A previous study in our group demonstrated that combining AmB with itraconazole with a similar oral drug delivery strategy elicited a pharmacological effect leading to drug concentrations above the minimum inhibitory concentration in liver and spleen for AmB⁹. In this case, MLT is more water soluble than itraconazole so we expect an enhanced oral absorption of AmB. However, further *in vivo* pharmacokinetic studies need to be carried out to confirm this hypothesis.

In terms of chemical stability and *in vivo* efficacy, it has been acknowledged that the coated formulations did not outperform F1. However, the inclusion of the coating provided a mechanism for sustained release of AmB, which might be beneficial for maintaining therapeutic drug levels over time, potentially improving the efficacy and safety of the treatment. Although the dissolution rates obtained *in vitro* were slower, this could help mitigate the adverse effects associated with the rapid release of AmB, improving overall patient compliance by reducing the frequency of dosing.

These results collectively suggested that AmB-MLT FDC granules could represent a valuable approach for treating VL orally. The ability to significantly reduce parasite burden combined with good gastrointestinal tolerability indicates that the oral treatment could be prolonged over 7 days aiming for a better pharmacological response. The oral administration of these formulations, thus, offers a convenient alternative to traditional parenteral AmB formulations, potentially improving patient compliance and treatment accessibility.

5. CONCLUSIONS

The development of oral AmB-MLT FDC granules represents a significant advancement in the treatment of VL. This approach offers several advantages over traditional intravenous AmB administration. Firstly, it provides a more patient-friendly treatment option that eliminates the need for hospitalisation, a crucial benefit in developing countries where healthcare resources are often limited. The formulations demonstrated remarkable stability for at least one year and showed promising results against two *Leishmania* species. *In vivo* studies rendered encouraging results, with a 65-80% reduction in parasite burden in the liver and spleen, which are the primary sites of accumulation in VL. Furthermore, the increase in body weight after the 7-day treatment course suggests that the formulation is well-tolerated for oral administration, with no apparent gastrointestinal toxicity. These findings collectively indicate that oral AmB-MLT FDC granules could be a game-changing approach in clinical practice for VL treatment, offering improved patient compliance, accessibility and potentially better therapeutic outcomes.

6. ACKNOWLEDGEMENTS

This work was funded by Banco de Santander-Universidad Complutense (project PR26/16-20355) and by the Iberoamerican Union of Universities (project ENF03/2017), awarded to F. Bolás-Fernández. A.M. Healy acknowledges a Science Foundation Ireland grant co-funded under the European Regional Development Fund (SFI/12/RC/22275_P2). This study has also been funded by the Ministry of Science and Innovation (award PID2021-126310OA-I00 to D.R. Serrano). Part of this study was funded by São Paulo Research Foundation (FAPESP), LIM50-FMUSP and the National Council for Scientific Development (CNPq) (grant number 2023/01641-1), awarded to L.F.D. Passero and M.D. Laurenti.

7. REFERENCES

1. Das, A.; Karthick, M.; Dwivedi, S.; Banerjee, I.; Mahapatra, T.; Srikantiah, S.; Chaudhuri, I., Epidemiologic Correlates of Mortality among Symptomatic Visceral Leishmaniasis Cases: Findings from Situation Assessment in High Endemic Foci in India. *PLOS Neglected Tropical Diseases* **2016**, *10* (11), e0005150.
2. Chappuis, F.; Sundar, S.; Hailu, A.; Ghalib, H.; Rijal, S.; Peeling, R. W.; Alvar, J.; Boelaert, M., Visceral leishmaniasis: what are the needs for diagnosis, treatment and control? *Nature Reviews Microbiology* **2007**, *5* (11), 873-882.
3. Fortún, J., [Antifungal therapy update: new drugs and medical uses]. *Enferm Infecc Microbiol Clin* **2011**, *29 Suppl 5*, 38-44.
4. van Griensven, J.; Balasegaram, M.; Meheus, F.; Alvar, J.; Lynen, L.; Boelaert, M., Combination therapy for visceral leishmaniasis. *Lancet Infect Dis* **2010**, *10* (3), 184-94.
5. van Griensven, J.; Boelaert, M., Combination therapy for visceral leishmaniasis. *Lancet* **2011**, *377* (9764), 443-4.
6. Bell, D. S., Combine and conquer: advantages and disadvantages of fixed-dose combination therapy. *Diabetes Obes Metab* **2013**, *15* (4), 291-300.
7. Mazon, P.; Galve, E.; Gomez, J.; Gorostidi, M.; Gorriz, J. L.; Mediavilla, J. D.; en representacion de las Sociedades Espanolas de Cardiologia, M. I. y. N., [Medical expert consensus in AH on the clinical use of triple fixed-dose antihypertensive therapy in Spain]. *Hipertension y riesgo vascular* **2016**.
8. Fernández-García, R.; Prada, M.; Bolás-Fernández, F.; Ballesteros, M. P.; Serrano, D. R., Oral Fixed-Dose Combination Pharmaceutical Products: Industrial Manufacturing Versus Personalized 3D Printing. *Pharm Res* **2020**, *37* (7), 132.
9. Fernández-García, R.; Walsh, D.; O'Connell, P.; Slowing, K.; Raposo, R.; Paloma Ballesteros, M.; Jiménez-Cebrián, A.; Chamorro-Sancho, M. J.; Bolás-Fernández, F.; Healy, A. M.; Serrano, D. R., Can amphotericin B and itraconazole be co-delivered orally? Tailoring oral fixed-dose combination coated granules for systemic mycoses. *European journal of pharmaceutics and biopharmaceutics : official journal of Arbeitsgemeinschaft fur Pharmazeutische Verfahrenstechnik e.V* **2023**, *183*, 74-91.
10. Mazza, A.; Schiavon, L.; Zuin, M.; Lenti, S.; Ramazzina, E.; Rubello, D.; Casiglia, E., Effects of the Antihypertensive Fixed-Dose Combinations on an Early Marker of Hypertensive Cardiac Damage in Subjects at Low Cardiovascular Risk. *American journal of hypertension* **2016**.
11. Kim, S. S.; Kim, I. J.; Lee, K. J.; Park, J. H.; Kim, Y. I.; Lee, Y. S.; Chung, S. C.; Lee, S. J., Efficacy and Safety of Sitagliptin/Metformin Fixed-Dose Combination Compared with Glimepiride in Patients with Type 2 Diabetes: A Multicenter, Randomized, Double-Blind Study. *Journal of diabetes* **2016**.
12. Everson, G. T.; Sims, K. D.; Thuluvath, P. J.; Lawitz, E.; Hassanein, T.; Rodriguez-Torres, M.; Desta, T.; Hawkins, T.; Levin, J. M.; Hinestrosa, F.; Rustgi, V.; Schwartz, H.; Younossi, Z.; Webster, L.; Gitlin, N.; Eley, T.; Huang, S. P.; McPhee, F.; Grasela, D. M.; Gardiner, D. F., Daclatasvir + asunaprevir + beclabuvir +/- ribavirin for chronic HCV genotype 1-infected treatment-naive patients. *Liver international : official journal of the International Association for the Study of the Liver* **2016**, *36* (2), 189-97.
13. Sundar, S.; Rai, M.; Chakravarty, J.; Agarwal, D.; Agrawal, N.; Vaillant, M.; Olliaro, P.; Murray, H. W., New treatment approach in Indian visceral leishmaniasis: single-dose liposomal amphotericin B followed by short-course oral miltefosine. *Clin Infect Dis* **2008**, *47* (8), 1000-6.
14. Ching, M. S.; Raymond, K.; Bury, R. W.; Mashford, M. L.; Morgan, D. J., Absorption of orally administered amphotericin B lozenges. *Br. J. Clin. Pharmacol.* **1983**, *16* (1), 106-108.
15. Torrado, J. J.; Serrano, D. R.; Uchegbu, I. F., The oral delivery of amphotericin B. *Ther Deliv* **2013**, *4* (1), 9-12.
16. Serrano, D. R.; Lalatsa, A., Oral amphotericin B: The journey from bench to market. *Journal of Drug Delivery Science and Technology* **2017**, *42*, 75-83.

17. Serrano, D. R.; Lalatsa, A.; Dea-Ayuela, M. A.; Bilbao-Ramos, P. E.; Garrett, N. L.; Moger, J.; Guarro, J.; Capilla, J.; Ballesteros, M. P.; Schätzlein, A. G.; Bolás, F.; Torrado, J. J.; Uchegbu, I. F., Oral particle uptake and organ targeting drives the activity of amphotericin B nanoparticles. *Mol Pharm* **2015**, *12* (2), 420-31.
18. Monge-Maillo, B.; López-Vélez, R., Miltefosine for Visceral and Cutaneous Leishmaniasis: Drug Characteristics and Evidence-Based Treatment Recommendations. *Clinical Infectious Diseases* **2015**, *60* (9), 1398-1404.
19. Pandey, K.; Ravidas, V.; Siddiqui, N. A.; Sinha, S. K.; Verma, R. B.; Singh, T. P.; Dhariwal, A. C.; Das Gupta, R. K.; Das, P., Pharmacovigilance of Miltefosine in Treatment of Visceral Leishmaniasis in Endemic Areas of Bihar, India. *Am J Trop Med Hyg* **2016**, *95* (5), 1100-1105.
20. Sundar, S.; Olliaro, P. L., Miltefosine in the treatment of leishmaniasis: Clinical evidence for informed clinical risk management. *Ther Clin Risk Manag* **2007**, *3* (5), 733-40.
21. Fernández-García, R.; de Pablo, E.; Ballesteros, M. P.; Serrano, D. R., Unmet clinical needs in the treatment of systemic fungal infections: The role of amphotericin B and drug targeting. *Int J Pharm* **2017**, *525* (1), 139-148.
22. Torrado, J. J.; Espada, R.; Ballesteros, M. P.; Torrado-Santiago, S., Amphotericin B formulations and drug targeting. *Journal of pharmaceutical sciences* **2008**, *97* (7), 2405-25.
23. Fernandez-Garcia, R.; Munoz-Garcia, J. C.; Wallace, M.; Fabian, L.; Gonzalez-Burgos, E.; Gomez-Serranillos, M. P.; Raposo, R.; Bolas-Fernandez, F.; Ballesteros, M. P.; Healy, A. M.; Khimyak, Y. Z.; Serrano, D. R., Self-assembling, supramolecular chemistry and pharmacology of amphotericin B: Poly-aggregates, oligomers and monomers. *J Control Release* **2022**, *341*, 716-732.
24. Pinto-Martinez, A. K.; Rodriguez-Duran, J.; Serrano-Martin, X.; Hernandez-Rodriguez, V.; Benaim, G., Mechanism of Action of Miltefosine on *Leishmania donovani* Involves the Impairment of Acidocalcisome Function and the Activation of the Sphingosine-Dependent Plasma Membrane Ca(2+) Channel. *Antimicrob Agents Chemother* **2018**, *62* (1).
25. Dorlo, T. P.; Balasegaram, M.; Beijnen, J. H.; de Vries, P. J., Miltefosine: a review of its pharmacology and therapeutic efficacy in the treatment of leishmaniasis. *J Antimicrob Chemother* **2012**, *67* (11), 2576-97.
26. Shanmugam, S., Granulation techniques and technologies: recent progresses. *Bioimpacts* **2015**, *5* (1), 55-63.
27. Cantor, S.; Augsburger, L.; Hoag, S.; Gerhardt, A., Pharmaceutical Granulation Processes, Mechanism and the Use of Binders. 2008; pp 261-301.
28. Wilkins, C. A.; Hamman, H.; Hamman, J. H.; Steenekamp, J. H., Fixed-Dose Combination Formulations in Solid Oral Drug Therapy: Advantages, Limitations, and Design Features. *Pharmaceutics* **2024**, *16* (2).
29. Espada, R.; Josa, J. M.; Valdespina, S.; Dea, M. A.; Ballesteros, M. P.; Alunda, J. M.; Torrado, J. J., HPLC assay for determination of amphotericin B in biological samples. *Biomedical Chromatography* **2008**, *22* (4), 402-407.
30. Serrano, D. R.; Walsh, D.; O'Connell, P.; Mugheirbi, N. A.; Worku, Z. A.; Bolas-Fernandez, F.; Galiana, C.; Dea-Ayuela, M. A.; Healy, A. M., Optimising the in vitro and in vivo performance of oral cocrystal formulations via spray coating. *European Journal of Pharmaceutics and Biopharmaceutics* **2018**, *124*, 13-27.
31. Serrano, D. R.; O'Connell, P.; Paluch, K. J.; Walsh, D.; Healy, A. M., Cocrystal habit engineering to improve drug dissolution and alter derived powder properties. *Journal of Pharmacy and Pharmacology* **2016**, *68* (5), 665-677.
32. Serrano, D. R.; Persoons, T.; D'Arcy, D. M.; Galiana, C.; Dea-Ayuela, M. A.; Healy, A. M., Modelling and shadowgraph imaging of cocrystal dissolution and assessment of in vitro antimicrobial activity for

sulfadimidine/4-aminosalicylic acid cocrystals. *European Journal of Pharmaceutical Sciences* **2016**, *89*, 125-136.

33. Smith, L.; Serrano, D. R.; Mauger, M.; Bolás-Fernández, F.; Dea-Ayuela, M. A.; Lalatsa, A., Orally Bioavailable and Effective Buparvaquone Lipid-Based Nanomedicines for Visceral Leishmaniasis. *Mol Pharm* **2018**, *15* (7), 2570-2583.

34. Serrano, D. R.; O'Connell, P.; Paluch, K. J.; Walsh, D.; Healy, A. M., Cocrystal habit engineering to improve drug dissolution and alter derived powder properties. *J Pharm Pharmacol* **2016**, *68* (5), 665-77.

35. Wolff, K., First-Order Elimination Kinetics. In *Encyclopedia of Psychopharmacology*, Stolerman, I. P., Ed. Springer Berlin Heidelberg: Berlin, Heidelberg, 2010; pp 536-536.

36. Paarakh, M. P.; Jose, P. A.; Setty, C. M.; Christopher, G. V. P., RELEASE KINETICS – CONCEPTS AND APPLICATIONS. *International Journal of Pharmacy Research & Technology* **2018**, *8*, 12-20.

37. Serrano, D. R.; Walsh, D.; O'Connell, P.; Mugheirbi, N. A.; Worku, Z. A.; Bolas-Fernandez, F.; Galiana, C.; Dea-Ayuela, M. A.; Healy, A. M., Optimising the in vitro and in vivo performance of oral cocrystal formulations via spray coating. *Eur J Pharm Biopharm* **2018**, *124*, 13-27.

38. Yoshioka, S.; Stella, V. J., Stability of Drugs and Dosage Forms. *Plenum, New York*, **2000**, 108-113.

39. de Pablo, E.; O'Connell, P.; Fernandez-Garcia, R.; Marchand, S.; Chauzy, A.; Tewes, F.; Dea-Ayuela, M. A.; Kumar, D.; Bolas, F.; Ballesteros, M. P.; Torrado, J. J.; Healy, A. M.; Serrano, D. R., Targeting lung macrophages for fungal and parasitic pulmonary infections with innovative amphotericin B dry powder inhalers. *Int J Pharm* **2023**, *635*, 122788.

40. Dea-Ayuela, M. A.; Castillo, E.; Gonzalez-Alvarez, M.; Vega, C.; Rolon, M.; Bolas-Fernandez, F.; Borrás, J.; Gonzalez-Rosende, M. E., In vivo and in vitro anti-leishmanial activities of 4-nitro-N-pyrimidin- and N-pyrazin-2-ylbenzenesulfonamides, and N2-(4-nitrophenyl)-N1-propylglycinamide. *Bioorganic & medicinal chemistry* **2009**, *17* (21), 7449-56.

41. Bilbao-Ramos, P.; Sifontes-Rodriguez, S.; Dea-Ayuela, M. A.; Bolas-Fernandez, F., A fluorometric method for evaluation of pharmacological activity against intracellular Leishmania amastigotes. *Journal of microbiological methods* **2012**, *89* (1), 8-11.

42. Evans, B. C.; Nelson, C. E.; Yu, S. S.; Beavers, K. R.; Kim, A. J.; Li, H.; Nelson, H. M.; Giorgio, T. D.; Duvall, C. L., Ex vivo red blood cell hemolysis assay for the evaluation of pH-responsive endosomolytic agents for cytosolic delivery of biomacromolecular drugs. *J Vis Exp* **2013**, (73), e50166.

43. Píneros, I.; Slowing, K.; Serrano, D. R.; de Pablo, E.; Ballesteros, M. P., Analgesic and anti-inflammatory controlled-released injectable microemulsion: Pseudo-ternary phase diagrams, in vitro, ex vivo and in vivo evaluation. *European Journal of Pharmaceutical Sciences* **2017**, *101*, 220-227.

44. Corral, M. J.; Serrano, D. R.; Moreno, I.; Torrado, J. J.; Domínguez, M.; Alunda, J. M., Efficacy of low doses of amphotericin B plus allicin against experimental visceral leishmaniasis. *Journal of Antimicrobial Chemotherapy* **2014**, *69* (12), 3268-3274.

45. Jesus, J. A.; da Silva, T. N. F.; Sousa, I. M. O.; Ferreira, A. F.; Laurenti, M. D.; da Costa, P. C.; de Carvalho Ferreira, D.; Passero, L. F. D., Nanostructured Lipid Carriers as Robust Systems for Lupeol Delivery in the Treatment of Experimental Visceral Leishmaniasis. *Pharmaceutics* **2023**, *16* (12), 1646.

46. Jesus, J. A.; Sousa, I. M. O.; da Silva, T. N. F.; Ferreira, A. F.; Laurenti, M. D.; Antonangelo, L.; Faria, C. S.; da Costa, P. C.; de Carvalho Ferreira, D.; Passero, L. F. D., Preclinical Assessment of Ursolic Acid Loaded into Nanostructured Lipid Carriers in Experimental Visceral Leishmaniasis. *Pharmaceutics* **2021**, *13* (6), 908.

47. Hall, A. V.; Gostick, I. E. F.; Yufit, D. S.; Marchant, G. Y.; Kirubakaran, P.; Madu, S. J.; Li, M.; Steel, P. G.; Steed, J. W., Integral Role of Water in the Solid-State Behavior of the Antileishmanial Drug Miltefosine. *Cryst Growth Des* **2022**, *22* (10), 6262-6266.

48. Lyu, F.; Liu, J. J.; Zhang, Y.; Wang, X. Z., Combined control of morphology and polymorph in spray drying of mannitol for dry powder inhalation. *Journal of Crystal Growth* **2017**, *467*, 155-161.

49. Park, N.-H.; Shin, K.-H.; Kang, M. K., 34 - Antifungal and Antiviral Agents. In *Pharmacology and Therapeutics for Dentistry (Seventh Edition)*, Dowd, F. J.; Johnson, B. S.; Mariotti, A. J., Eds. Mosby: 2017; pp 488-503.
50. Barakat, N. S.; Elbagory, I. M.; Almurshedi, A. S., Controlled-release carbamazepine granules and tablets comprising lipophilic and hydrophilic matrix components. *AAPS PharmSciTech* **2008**, *9* (4), 1054-62.
51. Dorlo, T. P. C.; Balasegaram, M.; Beijnen, J. H.; de Vries, P. J., Miltefosine: a review of its pharmacology and therapeutic efficacy in the treatment of leishmaniasis. *Journal of Antimicrobial Chemotherapy* **2012**, *67* (11), 2576-2597.
52. Ho, T.; Aris, R., On apparent second-order kinetics. *AIChE journal* **1987**, *33* (6), 1050-1051.
53. Mahajan, R.; Das, P.; Isaakidis, P.; Sunyoto, T.; Sagili, K. D.; Lima, M. A.; Mitra, G.; Kumar, D.; Pandey, K.; Van Geertruyden, J. P.; Boelaert, M.; Burza, S., Combination Treatment for Visceral Leishmaniasis Patients Coinfected with Human Immunodeficiency Virus in India. *Clin Infect Dis* **2015**, *61* (8), 1255-62.